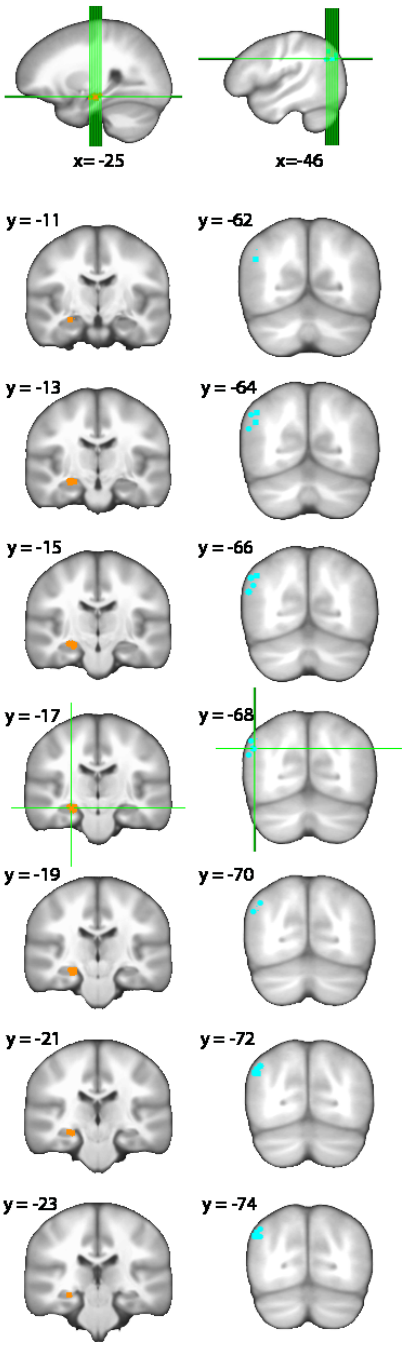

Figure S1. Individualized hippocampal seed locations and parietal stimulation targets. Related to Figure 1. Participant-specific hippocampal targets (orange) and parietal cortex stimulation locations (blue) visualized in stereotactic space on an averaged template brain (ICBM452). The location of coronal slices is indicated by green lines in the sagittal slice at the top of each column.

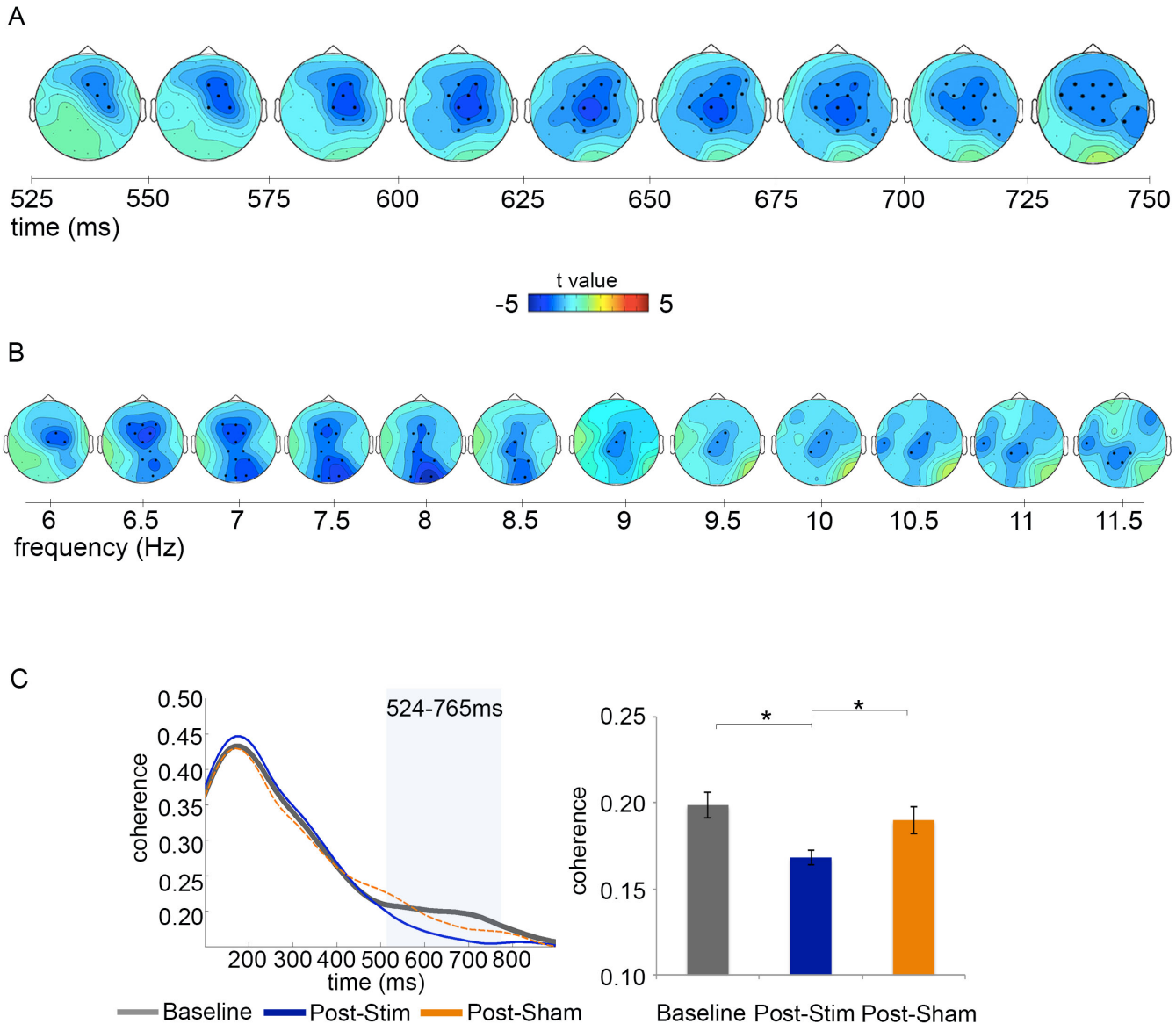

Figure S2. Power Reduction Post-Stim. Related to Figure 2. A. Fronto-parietal distributed power reduction Post-Stim relative to Baseline displayed as *t* value topographies in 25ms intervals from 525ms-750ms. B. *t* value topographies displaying significant frequencies x electrodes of Post-Stim compared to Baseline defined via cluster detection between 500-700ms. Electrodes included in the significant clusters are indicated by an *. C. Average inter-trial coherence (from 4-13Hz) is displayed across the epoch from 100-900ms. Bar plot displays mean coherence (and standard error) across 524-765ms time window, which is reduced Post-Stim (blue) compared to Baseline (gray) and Post-Sham (orange). *p<0.05

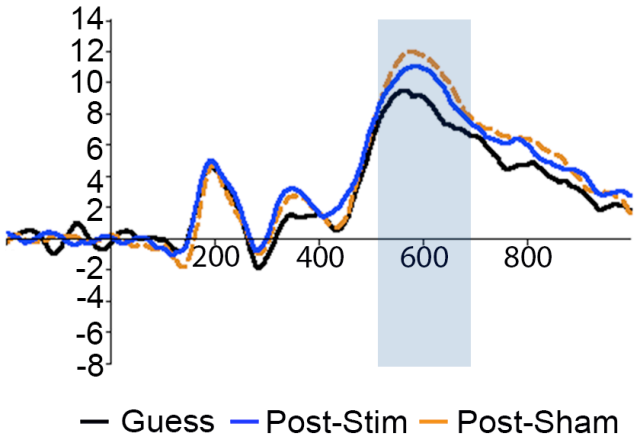

Figure S3. **Memory-related ERPs.** Related to Figure 3. ERPs time-locked to object cue at retrieval for Successful Post-Stim trials (blue), Successful Post-Sham trials (orange) and Guess trials (black) for electrode Pz. Average amplitude of posterior electrodes was compared across conditions for 500-700 ms.

		Recollection Success	Guess
Stimulation	Pre	2.38 (0.09)	8.69 (0.43)
	Post	2.19 (0.07)	9.41 (0.35)
Sham	Pre	2.26 (0.09)	9.49 (0.29)
	Post	2.30 (0.06)	9.20 (0.26)

Table S1. Raw distance error. Related to Figure 1. Mean raw distance error values in cm (and standard error) for n=12 subjects reported in primary analyses.

Supplemental Experimental Procedures

Participants:
Sixteen adults (mean age=25.7, range: 19-35 years; 11 female) participated in the experiment and were recruited based on no present use of psychoactive drugs and no history of neurological or psychiatric conditions. Participants were screened for MRI and TMS safety using standard MRI safety screening questionnaires and a TMS safety questionnaire [S1]. No participants withdrew due to complications or side effects. All participants gave written informed consent and were monetarily compensated for their time. Study procedures were approved by the Institutional Review Board at Northwestern University.

Twelve participants (mean age=25.3, range: 19-35 years; 9 female) were included in main analyses, and the same patterns of effects on location recall were identified for the entire sample. Two participants were excluded due to poor overall performance in which only 26.3% and 20.6% of trials, respectively, could be considered "successful recollection" (compared to 67.5% for all other participants). Few recollection trials coupled with poor EEG data quality yielded too-few trials for EEG/ERP analysis. Two additional participants were excluded for outlier change values across the week: precision was improved by 29.47% for one participant and reduced by -29.25% for the other participant relative to their Pre-Stim and Pre-Sham performance. These changes were over 2.5 standard deviations from the group mean and were therefore not likely due to stimulation, but rather to noise-related performance variability. Thus, including these subjects in the EEG/ERP analysis would reduce the ability to identify neural correlates of stimulation-related memory changes. Analysis of behavioral effects including all participants (N=16) were consistent with the primary effects reported for n=12. As stated in the main text, percent-improvement Post-Stim (mean=7.31%, se=3.54%) and percent-improvement Post-Sham (mean=2.6%, se=2.2%) were significantly different ($t(15)=2.89$, $p=0.01$; Cohen's d=0.72). Stimulation improved recall precision ($t(15)=2.38$, $p=0.03$; Cohen's d=0.60) whereas Sham had no significant effect ($t(15)=1.31$, $p=0.21$). Memory improvements were highly consistent due to Stim (15/16 participants showed precision improvements; Sign Test: $p=0.0005$), but were only at chance due to Sham (7/16 participants; Sign Test: $p=0.80$).

Experimental Design:
The Stim and Sham weeks (Figure 1C) were separated by an interval of at least 4 weeks (mean delay interval=12.62 weeks, range: 4.5 – 26.1 weeks). Twenty-four hours before and after the 5 consecutive daily stimulation sessions for each week, participants completed the memory task while EEG was recorded. The Stim and Sham weeks were administered in counterbalanced order across participants. As the experimental design was single blind, participants were not given information related to hypotheses concerning differential memory effects of Stim versus Sham. One hundred and ninety-two unique color drawings of objects[S2]were used as stimuli for each week (Stim and Sham). Half of the objects (96) were randomly assigned to each memory assessment session (Pre and Post), and an assessment-unique randomly assigned location was used for each object (retention of object-location associations across each week was thus not assessed in this experiment).

During each assessment session, participants completed an object-location memory task involving four study-test blocks. During each block (Figure 1A), participants viewed 24 objects presented at randomized locations on a blue-red-gray background grid (52.00 x 29.25 cm), viewed with an eye-to-screen distance of ~24 inches. Objects were presented one at a time for 3000 ms each (1000-ms ISI). Objects were presented within a white-box background (4.88 x 4.88 cm) and had a red dot superimposed at the object center to mark the precise location. Participants were instructed to study and remember the object-locations as accurately and precisely as possible. After each study phase, participants played a visuospatial "Tetris" distractor task [S3] for 90 s. After this delay, a cued-recall test was administered. During the test, the 24 studied objects were presented one at a time in the center of the screen (in a randomized order), and participants were required to recall the studied locations. At the beginning of every trial, a gray screen with the letter "b" in the center of the screen appeared for 2000 ms. Participants were encouraged to blink freely during this period (and limit blinking for the remainder of the trial). This period was followed by a 2000 ms fixation cross at the center of the screen. Then, an object appeared at the center of the screen for 2000 ms. During this time, participants were instructed to focus on the object, and mentally recall its studied location. After this 2000 ms period, participants were able to use the mouse to move the object from the center of the screen to its recalled location and click a button on the mouse to indicate its final location.

Behavioral analysis:
Statistical analyses were done in R [S4]. The distance threshold for successful recollection was determined using three converging approaches. First, the size of objects used during memory testing was 4.88x4.88 cm, and therefore in the context of our specific task "successful recollection" refers to accuracy within one stimulus length from the studied location. Second, we applied thresholds for recollection success taken from modeling results using a word-location association task [S5, S6]. Harlow and Yonelinas (2016) used growth-mixture modeling to fit a Cauchy distribution (for successful recollection) and a uniform distribution (for random guessing) to distance errors in a radial location recall task. The modeling results in two parameters: a mixture parameter (λ) denoting the proportion of success relative to guess, and a shape parameter (s) denoting precision. The mixture parameter indicated that the most accurate 65% of trials fit the Cauchy distribution and could be

considered successful recollection. For all assessment conditions and all participants (N=16), this 65% threshold corresponds to 5.41 cm in our data. Finally, we used a similar mixture-modeling approach to fit Cauchy and null distributions to distance errors in the current task, aggregated across all four testing sessions and all participants. This model provided a good fit to the distance error data (p=0.24, where p<0.05 would indicate poor fit) and indicated that 64.64% of trials fit the Cauchy distribution, which across all participants corresponded to 5.36 cm. Thus, these approaches all converge on about 65% as a reasonable threshold for successful recollection. Notably, random placement of the object during memory testing would yield successful recollection for about 5.4% of trials, and so actual performance was about ten-fold higher than would be expected by chance. Within the successfully recollected trials, we defined precision as the mean error of these trials.

It is important to note that random locations were selected for all objects at study, and therefore not all objects had equal error probability. For example, an object studied at an outer corner has a greater probability of higher error because its distance to all other points on the screen is greater than an object studied at the center. We excluded all trials with error greater than 19.5 cm in analyses to account for outlier values that would result from guess responses on trials with high error possibility. This left a total of 4,330 trials (93.97%) across all assessment sessions for final analysis. Excluding outlier trials within the n=12 sample used in primary analyses, the 4.88-cm cutoff resulted in an average of 67.56% (se=4.47%) successful recollection trials across all assessment conditions. Cohen's d effect size [S7] tests are reported in conjunction with significant results.

A common Baseline including Pre-Stim and Pre-Sham distance error values was used for primary analyses, although effects remained consistent when using separate Pre-Stim and Pre-Sham values as baselines for each experimental week. Distance errors were slightly yet significantly greater Pre-Stim compared to Pre-Sham (t(11)=2.40, p=0.036, Cohen's d=0.690) (Table S1). Importantly, the primary analyses showed that Post-Stim mean error was significantly less than Post-Sham, and improvement for Stim therefore cannot be attributed to greater room for improvement for the Stim condition compared to the Sham condition or by so-called "regression to the mean". That is, despite Stim starting off slightly significantly worse than Sham, after stimulation it was significantly better. Furthermore, all primary analyses used a common Baseline in conjunction with a within-subject counterbalanced design to counteract any interpretation related to practice effects or baseline differences. We also calculated percent-improvement of precision using individual Pre-Stim and Pre-Sham performance (Figure 1GH). Percent-improvement for Post-Stim versus Pre-Stim (mean=7.64%, se=1.65%) was significantly greater (t(11)=3.70, p=0.004; Cohen's d=1.07) compared to Post-Sham versus Pre-Sham (mean=-2.7%, se=2.58%). Stim improved recall precision relative to Pre-Stim baseline (t(11)=4.6266, p=0.0007; Cohen's d=1.34) whereas Sham did not improve precision relative to Pre-Sham baseline (t(11)=1.042, p=0.32). Overall, the effects of stimulation were greater when measured using individual-week baseline values rather than the common baseline used for primary analyses. For precision behavioral analyses, an average of 66.6 (sd=13.79) trials Pre-Stim, 61.8 (sd=16.14) trials Pre-Sham, 128.4 (sd=27.06) trials Baseline, 67.2 (sd=14.68) trials Post-Stim and 63.8 (sd=15.96) trials Post-Sham were used.

To further establish the specificity of this effect, we assessed effects on distance error for guess trials. Relative to baseline, Post-Stim (mean=4.1%, se=3.9%) compared to Post-Sham (mean=1.9%, se=3.1%) was not significantly different (t(11)=0.55, p=0.59). Neither Stim (t(11)=1.05, p=0.32) nor Sham (t(11)=0.60, p=0.56) improved distance error relative to Baseline for guess trials. Therefore, effects of stimulation did not occur on guesses.

Stimulation target identification:

We determined an individualized left lateral parietal stimulation location based on high resting-state fMRI connectivity with a left hippocampal seed using the same methods as in Wang et al. 2014 [S8]. MRI data were collected using a Siemens 3T TIM Trio whole-body magnet with a 32-channel head coil, provided by Northwestern University Center for Translational Imaging (CTI) Facility, supported by Northwestern University Department of Radiology. To provide anatomical localization for stimulation, a structural and resting-state scan was performed prior to any other memory assessment on the first day of participation. A MPRAGE T1-weighted structural image was acquired (with TR=2400 ms, TE=3.16 ms, FOV=25.6 cm, flip angle=8°, and 1mm^3 voxel resolution over 176 sagittal slices). Functional resting-state images were acquired using a whole-brain BOLD EPI sequence (with TR=2500 ms, TE=20 ms, FOV=22 cm, flip angle=80°, and 1.72x1.72x3-mm voxel resolution over 244 volumes). During the 10.2-min resting-state scan, participants were instructed to lie still with their eyes open. Functional and structural MRI data were preprocessed using AFNI [S9]. Preprocessing included motion correction, slice-timing correction (to the first slice), functional-structural co-registration, resampling to a resolution of 1.5x1.5x1.5 mm, stereotactic transformation using Montreal Neurologic Institute 305 (MNI-305) template, band-pass filtering (0.01-0.10Hz), spatial smoothing (with a 4-mm FWHM Guassian kernel), despiking, linear de-trending, and regressing out the motion time-series. A hippocampal seed voxel was located for each participant by identifying a voxel in the middle of the body nearest to MNI [-24, -18, -18] (mean distance away=6.82 mm, se=0.49). The fMRI time course data were extracted from the hippocampal seed voxel and used in a seed-based resting-state functional connectivity analysis. We identified a cluster of voxels in the left parietal cortex exhibiting the maximum connectivity within a 15 mm radius (mean=8.32 mm, se=1.04) nearest to MNI [-47, -68, 36], which was used as the Stim location. A Sham stimulation location (the vertex) was located at the MNI coordinate [0, -42, 73]. The stimulation location target for Stim and Sham were transformed from MNI space into each participant's original MRI space for anatomically guided rTMS.

rTMS:
Nexstim eXimia NBS 4.3 air-cooled MRI Guided system (Nexstim Ltd., Helsinki, Finland) with a 70-mm figure-of-eight coil was used to apply stimulation to targeted locations marked on the structural MRI using a frameless infrared stereotactic system. Motor Threshold (MT) was determined on the first day of participation, which was defined as the minimum stimulator output required to generate a contraction of the *abductor pollicis brevis* for 5 consecutive pulses measured either visually or via EMG contraction threshold of 50 mV. rTMS was applied at 100% MT for both Stim and Sham. For two participants, stimulation over the targeted parietal location was applied at a lower intensity (89% MT for one, and 83% MT for the other) due to reported mild discomfort for 100% MT on the first day of repetitive stimulation. The rTMS protocol consisted of 20 minutes of consecutive blocks of 20-Hz pulses for 2 s, followed by 28 s of no stimulation (1,600 pulses per session).

EEG:
Continuous EEG was recorded during the test phase from 30 scalp channels (amplifier bandwidth DC to 20,000 Hz, sampled at 1,000 Hz) using active Ag/AgCl electrodes (Brain Vision LLC, actiCAP). Mean impedance across all electrodes and assessment sessions was < 10 kΩ. EEG signals were amplified and digitized online. The right mastoid was used as an online reference. The recordings were then re-referenced offline to the left and right mastoid. Electrooculography (EOG) was also used to monitor eye-movements and blinks. Bipolar electrodes at the left and right outer canthi, as well as above and below the right eye were recorded. A high-pass filter (0.1 Hz, 12 dB per octave) was applied to all channels prior to any analysis. Trials with ocular artifacts (large voltage offsets identified in 200-ms moving windows for each participant ranging between 6-20 mV) were removed from all analyses. An additional absolute voltage threshold (defined individually for each participant ranging between 100-200 μV) was applied when necessary to scalp electrodes to identify and subsequently remove trials dominated by muscle activity or movement. As with our behavioral data, our main EEG analyses concerned changes due to stimulation (Post-Stim versus Baseline) relative to control (Post-Sham versus Baseline).

Time-frequency decomposition and statistical analyses were performed using FieldTrip [S10]. EEG data were epoched from -500 to 1500 ms relative to onset of the object presentation during cued-recall. For each condition, evoked oscillations were obtained via time-frequency decomposition of baseline corrected event-related averages using Mortlet wavelets (width=5) in 0.5 Hz increments of 2-30 Hz over the entire epoch in 1-ms steps with a Hanning taper. Power was analyzed with non-parametric cluster-based permutation tests[S11], for the frequency band from 4-13 Hz in a latency interval of 0 to 1000 ms. For all contrasts, a channel x time dependent *t*-test was conducted for each individual sample. To control for multiple comparisons, a Monte Carlo estimate of the permutation *p*-value was calculated by randomly permuting condition comparisons over 1000 iterations. Clusters were considered significant at $p<0.05$. As with the behavioral analysis, we collapsed trials across Pre-Stim and Pre-Sham sessions as a common Baseline for each individual. Only successfully recollected trials were included in analyses. After artifact rejection, an average of 97.00 trials (range: 56-137) trials were included in Baseline, 53.91 (range: 28-69) trials were included in the Post-Stim condition and 48.75 (range: 25-66) trials were included in the Post-Sham condition. The number of trials included Post-Stim and Post-Sham did not differ significantly ($t(11)=0.63$, $p=0.54$). As stated in the main text, this analysis yielded a significant power reduction (Figure 2ABC) for 524-765ms for Post-Stim compared to Baseline (*cluster corrected* $p=0.03$) for a subset of fronto-parietally distributed electrodes including FZ, F3, F4, F8, FC1, FC2, FC5, FC6, CZ, C3, C4, CP1, CP2, CP5, CP6, PZ, P8, T8 (Figure S2A). No significant cluster was found for Post-Sham compared to Baseline. EEG oscillatory effects remained consistent irrespective of choice of baseline. 4-13Hz power averaged over 524-765ms was significantly reduced Post-Stim relative to Pre-Stim baseline ($t(11)=2.45$, $p=0.032$), but remained unchanged Post-Sham relative to Pre-Sham baseline ($t(11)=0.16$, $p=0.876$).

To identify oscillatory changes apart from the a priori 4-13Hz range, power was also analyzed with a non-parametric cluster-based permutation test [S11], averaged for 500-700ms after event onset, given a range of 2-30Hz. This latency interval was chosen because late EEG oscillatory correlates (>500ms after event onset) are thought to relate to recollection of spatial context information[S12, S13, S14]. For all contrasts, a channel x frequency dependent t-test was conducted for each individual sample. To control for multiple comparisons, a Monte Carlo estimate of the permutation p value was calculated by randomly permuting condition comparisons over 1,000 iterations, with a cluster corrected significance criterion of $p < 0.05$. The analysis comparing Post-Stim to Baseline yielded a significant reduction (*cluster-corrected* $p=0.02$) across 6-11.5Hz (Figure S2B) in a subset of electrodes (OZ, O1, O2, PZ, P4, CZ, CP1, CP2, FC1, FC2, FZ, F3, F4). This frequency range found via cluster-detection was consistent with the theta-alpha a priori frequency range used for primary analyses, confirming that theta-alpha oscillatory activity correlates of recollection were reduced due to stimulation.

To measure the phase consistency across trials, inter-trial phase coherence (ITPC) was calculated for each condition averaged across 4-13Hz (Figure S2C). ITPC for the 524-765ms latency interval was significantly reduced Post-Stim compared to Baseline ($t(11) = 3.85$, $p=0.003$, Cohen's d=1.11) and compared to Post-Sham($t(11)=2.28$, $p=0.04$, Cohen's d=0.66), whereas there was no change Post-Sham compared to Baseline ($t(11)=0.71$, $p=0.49$).

Event-related potentials (ERP) analysis was conducted using ERPlab [S15]. For ERP analyses, EEG data were re-epoched from -200 to 1000ms (shorter baseline was used here to improve trial counts, as longer baselines are not needed for ERPs). Each trial was baseline corrected using the pre-stimulus interval. Based on many previous ERP studies of successful recollection[S12, S14, S16, S17], we first confirmed that our recall task evoked standard neural correlates of recollection. We compared ERP mean amplitude for successful memory Post-Stim and Post-Sham compared to a Guess condition (guess trials collapsed across Post-Stim and Post-Sham to ensure sufficient trial counts) for 500-700 ms at the same posterior electrodes used in primary analyses (Figure S3). Repeated-measures ANOVA of average amplitude used *condition* as a factor (success Post-Stim, success Post-Sham, and Guess). There was a main effect of condition ($F(2,22)=5.64$, $p=0.01$). ERPs were significantly greater for successful Post-Stim ($t(11)=2.35$, $p=0.03$) and successful Post-Sham ($t(11)=3.25$, $p=0.008$). Relative to guess, Post-Stim ERPs had lesser amplitudes (mean amplitude difference =1.26 μV, se=0.53 μV) than Post-Sham ERPs (mean amplitude difference=1.849 μV, se=0.57 μV). Thus, comparison of recollection success versus guess for Post-Stim and Post-Sham confirmed reliable ERP correlates of successful recollection in our task, indicating that the reduced amplitudes reported in the primary analysis (Figure 3) reflected reduction of recollection-related neural signals.

An average of 107.9 (range: 64-144) trials were included in Baseline condition, 55.25 (range: 33-71) trials were included in Post-Stim condition and 57.8 (range: 29-71) trials were included in the Post-Sham condition. The number of trials included Post-Stim and Post-Sham did not differ significantly ($t(11)=0.86$, $p=0.41$). Our main analyses focused on the parietal memory effect[S12], which was quantified at nine central-posterior electrodes (CP1, CP2, CZ, P3, PZ, P4, O1, OZ, O2). To guard against possible outliers, a robust correlation was used to test the relationship between the parietal memory effect and percent precision improvement[S18]. For this correlation, we used the maximum amplitude reduction (Baseline-Post) among the central-posterior electrodes compared to the percent precision improvement calculated relative to Baseline. A 30 Hz low-pass filter was applied for waveform presentation only.

Zero-intensity Stimulation Control Experiment:
The primary experiment involved full-intensity stimulation of a network-defined parietal target (Stim) compared to full-intensity stimulation of an out-of-network vertex location (Sham). To evaluate whether reported effects were due to performance reductions in the Sham condition as opposed to performance enhancements in the Stim condition, we performed an additional control experiment involving near-zero intensity stimulation of network-defined parietal locations. For this control experiment, participants (N=12; mean age=24.6 years, range: 20-34 years; 8 female) received stimulation over the lateral parietal cortex using the same parameters as in the main experiment, except that a spacer was used to increase the distance between the coil and the target location such that the induced voltage at the stimulation location was effectively zero. The target location in the parietal cortex was determined based on functional connectivity of the posterior hippocampus using the same fMRI acquisition and analysis parameters as in the main experiment. Subjects received only zero-intensity control stimulation, and so participated one week only, using the same 5-day stimulation protocol with 24-hr pre- and post-testing, as in the main experiment.

As in the main experiment, successful recollection was defined as trials within 4.88 cm, and within successful recollection, precision was defined as mean distance error. We found no significant change in precision for Post-Control compared to Pre-Control ($t(11)=1.57$, $p=0.145$), and percent change (mean=5.39%, se=3.39%) was not different from zero ($t(11)=1.59$, $p=0.139$). Effects on precision memory were therefore specific to full-intensity stimulation to the lateral parietal cortex. Likewise, oscillatory neural correlates of precision were not significantly different Post-Control. To evaluate changes in theta-alpha power, a cluster-based simulation of 4-13Hz over the entire epoch revealed no significant time-electrode cluster ($p>0.3$). Averaged power over 4-13Hz for 524-765-ms latency interval used in the primary analysis also did not significantly differ between Pre-Control and Post-Control ($t(11)=1.73$, $p=0.11$). Furthermore, event-related mean amplitude (ERP) for successfully recollected trials was not significantly different Pre-Control versus Post-Control for the same latency interval ($t(11)=1.22$, $p=0.248$). Thus, precision memory improvement and an associated reduction of recollection neural correlates only occurred reliably for targeted HPM network stimulation (Stim), not for both control conditions.

Supplemental References

S1. Rossi, S., Hallett, M., Rossini, P.M., Pascual-Leone, A., and Safety of, T.M.S.C.G. (2009). Safety, ethical considerations, and application guidelines for the use of transcranial magnetic stimulation in clinical practice and research. Clin Neurophysiol *120*, 2008-2039.

S2. Rossion, B., and Pourtois, G. (2004). Revisiting Snodgrass and Vanderwart's object pictorial set: the role of surface detail in basic-level object recognition. Perception *33*, 217-236.

S3. Pfister, R. (2008). Pretris - Tetris for presentation. Archives of Neurobehavioral Experiments and Stimuli *198*.

S4. Team, R.D.C. (2008). R: A Language and Environment for Statistical Computing. (Vienna, Austria).

S5. Harlow, I.M., and Donaldson, D.I. (2013). Source accuracy data reveal the thresholded nature of human episodic memory. Psychon Bull Rev *20*, 318-325.

S6. Harlow, I.M., and Yonelinas, A.P. (2016). Distinguishing between the success and precision of recollection. Memory *24*, 114-127.

S7. J, C. (1992). Statistical Power Analysis for the Behavioral Sciences, 2nd Edition, (Lawrence Erlbaum Associates).

S8. Wang, J.X., Rogers, L.M., Gross, E.Z., Ryals, A.J., Dokucu, M.E., Brandstatt, K.L., Hermiller, M.S., and Voss, J.L. (2014). Targeted enhancement of cortical-hippocampal brain networks and associative memory. Science *345*, 1054-1057.

S9. Cox, R.W. (1996). AFNI: software for analysis and visualization of functional magnetic resonance neuroimages. Comput Biomed Res *29*, 162-173.

S10. Oostenveld, R., Fries, P., Maris, E., and Schoffelen, J.M. (2011). FieldTrip: Open source software for advanced analysis of MEG, EEG, and invasive electrophysiological data. Comput Intell Neurosci *2011*, 156869.

S11. Maris, E., and Oostenveld, R. (2007). Nonparametric statistical testing of EEG- and MEG-data. J Neurosci Methods *164*, 177-190.

S12. Rugg, M.D., and Yonelinas, A.P. (2003). Human recognition memory: A cognitive neuroscience perspective. Trends Cogn Sci *7*, 313-319.

S13. Spitzer, B., Hanslmayr, S., Opitz, B., Mecklinger, A., and Bauml, K.H. (2009). Oscillatory correlates of retrieval-induced forgetting in recognition memory. J Cogn Neurosci *21*, 976-990.

S14. Rugg, M.D., and Curran, T. (2007). Event-related potentials and recognition memory. Trends Cogn Sci *11*, 251-257.

S15. Lopez-Calderon, J., and Luck, S.J. (2014). ERPLAB: an open-source toolbox for the analysis of event-related potentials. Front Hum Neurosci *8*, 213.

S16. Bridge, D.J., and Paller, K.A. (2012). Neural correlates of reactivation and retrieval-induced distortion. J Neurosci *32*, 12144-12151.

S17. Van Petten, C., Senkfor, A.J., and Newberg, W.M. (2000). Memory for drawings in locations: spatial source memory and event-related potentials. Psychophysiology *37*, 551-564.

S18. Pernet, C.R., Wilcox, R., and Rousselet, G.A. (2012). Robust correlation analyses: false positive and power validation using a new open source matlab toolbox. Front Psychol *3*, 606.